Pramāṇa – J. Phys., Vol. 33, No. 5, November 1989, pp. 595–602. © Printed in India.

# Phonon density of states of tetracyanoethylene from coherent inelastic neutron scattering at Dhruva reactor

S L CHAPLOT, R MUKHOPADHYAY, P R VIJAYARAGHAVAN, A S DESHPANDE and K R RAO

Nuclear Physics Division, Bhabha Atomic Research Centre, Bombay 400 085, India

MS received 22 April 1989

**Abstract.** Inelastic neutron scattering experiments to determine phonon density of states of coherent scattering samples of polycrystalline complex solids are generally intensity-limited and therefore are feasible only at high flux facilities. Phonon density of states of the monoclinic phase of tetracyanoethylene at 300 K, obtained using the medium resolution triple axis spectrometer at the new Indian medium flux reactor Dhruva are reported here. The raw data is converted to the "neutron weighted" phonon density of states by applying suitable corrections. Comparison made with results from a theoretical calculation based on a semirigid molecule model of lattice dynamics is fair. Results from Dhruva are also consistent with that obtained (to be published) at the high flux pulsed neutron source (ISIS) of the Rutherford Appleton Laboratory in United Kingdom.

**Keywords.** Inelastic neutron scattering; phonon density of states; lattice dynamics; tetracyanoethylene.

**PACS Nos** 28·20; 63·20; 28·50

## 1. Introduction

The vibrational properties of solids are conveniently studied by the Raman scattering and the infrared absorption techniques. However, the information so obtained from such optical experiments in crystalline solids is often restricted to some of the long wavelength phonons which may be accessible by the selection rules. Inelastic neutron scattering is the unique technique (Chaplot 1986), which is widely used to obtain information on the phonons in the entire Brillouin zone. But large single crystals, which are often difficult to obtain, are needed in order to probe the individual phonons. Polycrystalline samples can be used, in principle, to obtain the density of phonon states. However, the observable neutron scattering intensities are usually very low, and the analysis of data is often difficult. The only exceptions are those samples which contain specific isotopic elements, especially hydrogen, which have large incoherent neutron scattering cross-sections. In such samples, however, the measured spectrum will be dominated by the vibrational states of the hydrogen-like elements only, and information about dynamics of other atoms will be missed.

Most atoms, other than that of hydrogen (i) have low cross-sections and (ii) scatter neutrons essentially coherently. Although there is no correlation between these two factors, they both lead to certain difficulties in the experiments. The low scattering cross-sections lead to poor inelastic neutron intensities at the low/medium neutron facilities (Roy and Brockhouse 1970). Coherent scattering introduces a wave vector

(Q) dependence in the inelastic structure factor $S(\mathbf{Q}, E)$. While such dependence may be gainfully exploited in a few cases (Carpenter and Price 1985; Maley *et al* 1986), in general, one has to suitably average $S(\mathbf{Q}, E)$ over a large Q-range to wipe out coherent effects of an already weak signal to obtain the density of states. The nature of Q-dependence becomes complicated while working with solids of complex structures.

Despite the above difficulties, there is convenience in using polycrystalline or powder samples, over the use of large single crystals. There are very few cases where medium flux reactors have been used to obtain density of phonon states of coherent scatterers. Therefore, it is important to establish the feasibility of measurement of phonon density of states of complex systems at medium flux reactor facilities like the Indian reactor Dhruva. Dhruva, has a maximum neutron flux of $1{\cdot}5 \times 10^{14}$ neutrons/cm$^2$/s, in comparison with the more advanced reactors like the high flux reactor at the Institute Laue-Langevin at Grenoble having a flux of about $1{\cdot}5 \times 10^{15}$ neutrons/cm$^2$/s.

The present experiments, on the monoclinic phase of tetracyanoethylene at 300 K, have been carried out using the triple axis spectrometer which is provided with a fully automatic on-line computer controlled data collection and operation system. Tetracyanoethylene has been of considerable interest to us due to its unusual phase transitions and phonon properties (Mukhopadhyay *et al* 1985; Chaplot and Mukhopadhyay 1986; Chaplot 1987; Sahu *et al* 1987). Experimental details are given in §2, followed by the results and analysis in §3 and a summary in §4. A brief report was presented elsewhere in a symposium (Chaplot *et al* 1988a).

## 2. Experimental

A schematic diagram of the triple axis spectrometer is given in figure 1. A Cu(111) monochromator is used to monochromatise thermal neutrons emerging from a

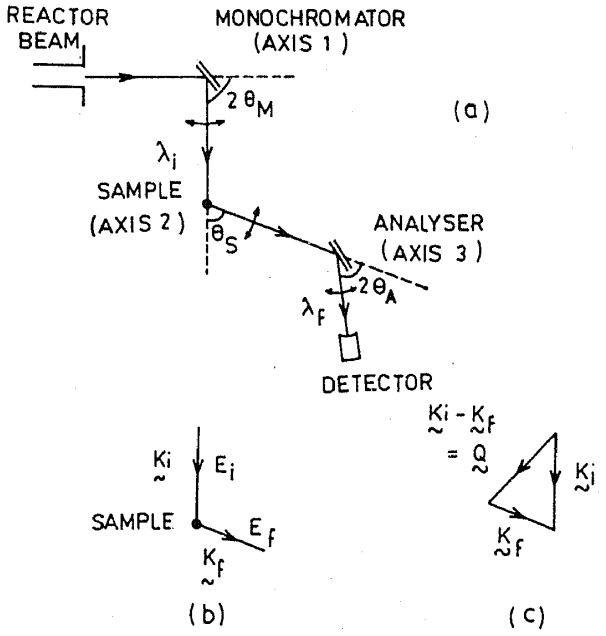


**Figure 1.** (a) Schematic diagram of triple axis spectrometer. (b) and (c) show the vectors $\mathbf{K}_i$, $\mathbf{K}_f$ and Q with respect to the spectrometer.

tangential beam tube ($T$ 1007) of the Dhruva reactor. By rotating the monochromator drum in a 2:1 ratio with respect to the monochromator, neutron beams of continuously variable incident wavelength are obtained. These monochromatic neutrons fall on the sample contained in a suitable sample holder and can be observed over a scattering angle range of 10° to 90°. The inelastically scattered neutrons are energy analyzed using a pyrolytic graphite (002) analyzer and the intensity of scattered neutrons as a function of energy is measured by a $BF_3$ detector. Angular collimators had divergence of 1° (FWHM) throughout the scattering geometry. The inelastic scattering experiments were performed with the neutrons, losing energy in the scattering process. The intensity of the spectrum on the neutron energy loss side is larger than that on its energy gain side by the ratio $\exp(E/kT)$. $E$ denotes the energy transfer, equal to $(E_i - E_f)$, where $E_i$ and $E_f$ are the incident and scattered neutron energies respectively.

The operation of the spectrometer is controlled by a on-line personal computer with the help of *user friendly* Fortran based programs. A variety of scans like a constant $Q$ scan with $E_i$ or $E_f$ fixed, or a constant $E$ scan, or a constant scattering angle scan with $E_i$ or $E_f$ fixed, can be carried out using a variety of application software available.

The energy scan can be made with either $E_i$ fixed or $E_f$ fixed. Both the arrangements were used for cross checking the data. In both cases the second order reflections from the monochromator and analyzer crystals pose difficulties.

A powder sample of the monoclinic phase of TCNE of volume of about 10 cc weighing nearly 10 g was used in a thin polythene container of size of about $5 \times 4 \times 0{\cdot}5$ cm.

Figure 2 shows the data with fixed $E_i$ equal to 44·6 meV at a fixed scattering angle of 40°. The two peaks at $\theta_A$ of 11·65° and 23·3° are due to the elastically scattered neutrons reflected by the PG(002) and PG(004) planes respectively. The neutrons observed in the range of $\theta_A$ of 11·65° to 23·3° correspond to the neutrons that have lost energy (i.e. $E > 0$) and reflected by PG(002) planes, and also those that have gained energy (i.e. $E < 0$) and reflected by PG(004) planes. A point-to-point analysis of the two possibilities, using the Boltzmann factor $\exp(-E/kT)$, shows that useful data can be extracted in the $E$ range of 0 to 25 meV. We also note that the second order

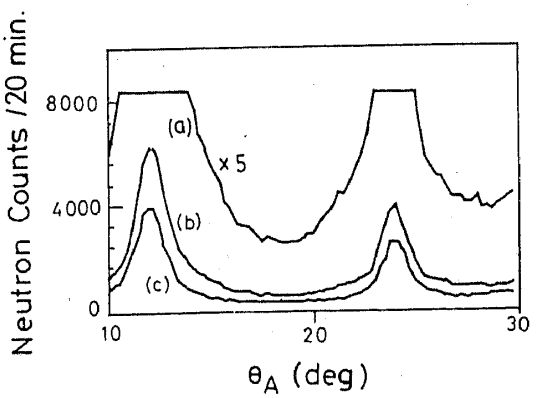


**Figure 2.** Observed neutron intensity from TCNE with $E_i$ and scattering angle $\theta_s$ held constant at 44·6 meV and 40° respectively. $Q$ varied between 2·9 and 3·3 $A^{-1}$ as a function of $E_f$. In (**a**) intensity is scaled up by a factor of 5 of the raw data shown in (**b**). (**c**) is the contribution due to sample container. Counting time at each point is approximately 20 min at full power of Dhruva reactor.

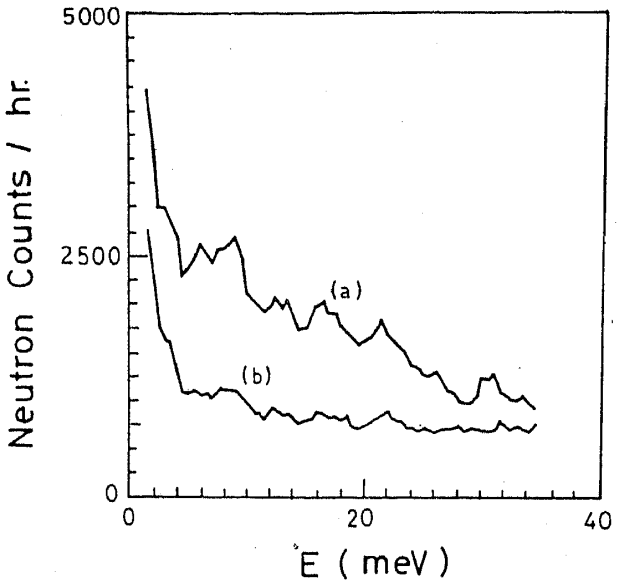


**Figure 3.** Observed neutron intensity from TCNE with $E_f$ and $Q$ held constant at 14·8 meV and 3 $A^{-1}$ respectively. The scattering angle varied from 30° to 67° as a function of varying $E_i$. (**a**) and (**b**) show raw data and background contribution from sample container respectively. Counting time at each point is approximately 1 h at full power of the Dhruva reactor.

reflection from the monochromator would occur for neutrons, of energy $4E_i$ equal to 178·4 meV, but such neutrons are relatively few in the reactor spectrum and are ignored here.

The experiment with fixed $E_f$ was carried out with $E_f = 14{\cdot}8$ meV. In this case, the second order neutrons of energy $4E_f (= 59{\cdot}2$ meV) are prevented from reaching the analyzer by placing a PG(002) filter in between the sample and the analyzer. Correction has, however, to be made for the second order reflection from the monochromator. Figure 3 gives the energy scan with fixed $E_f$ of 14·8 meV.

## 3. Data analysis and results

The scattered neutron intensity is proportional to the double differential scattering cross-section given by

$$d^2\sigma/(d\Omega\, dE) = \{K_f/K_i\} S(Q, E) \tag{1}$$

where $S(Q, E)$ is the dynamical structure factor. $\mathbf{Q}$ denotes the wave vector transfer, equal to $(\mathbf{K}_i - \mathbf{K}_f)$, where $\mathbf{K}_i$ and $\mathbf{K}_f$ are wave vectors of the incident and scattered neutrons respectively. However, to reduce the observed spectra, as in figures 2 and 3, to $S(Q, E)$, many corrections are needed. The corrections applied in this study are discussed briefly in the following:

(i) The background counts obtained with empty container in the sample position, are subtracted at each scan point from the total (signal + background) spectrum with suitable normalization to the same incident neutron intensity. The background

contributions from container thus normalized are shown in figures 2(c) and 3(b). (ii) Geometrical corrections are made for variations, from point-to-point in the scan, in the path length of the neutron through the flat sample due to any changes in the angle of incidence. Neutron absorption in the present case is estimated to be negligible. (iii) A geometrical correction is also applied for any change in the width of the neutron beam as one follows the path of the neutron from the monochromator to the detector. As the monochromator is rotated, variable width of beam falls on the monitor counter. Only a fraction of these neutrons may be incident on the sample. Further, only a fraction of the scattered neutron beam may be intercepted by the analyzer crystal. The overall correction due to this effect depends on the actual widths of the monochromator and analyzer crystals, the sample width and the angles $2\theta_M, \theta_s, \psi$, and $2\theta_A$ ($\psi$ is the angle defining the orientation of the flat sample with respect to the incident beam). (iv) Correction is made for the component of neutrons reflected in the second order from the monochromator and variation in the reflectivity of the monochromator with $E_i$. This correction is significant ($> 5\%$) only for $E_i < 27$ meV. (v) Variation in the reflectivity of the analyzer crystal with $E_f$ is also corrected. (vi) The scattered neutrons are usually counted for a fixed number of monitor counts. A monitor counter is placed in-between the monochromator and the sample and has a neutron efficiency proportional to $1/K_i$. Correction is applied for the variation in monitor efficiency with energy. Variations in the detector efficiency are much less significant. (vii) As shown by Dorner (1972), for our case with $K_f$ fixed and a $1/K_i$ monitor, no corrections for changing resolution are required. For the case with $K_i$ fixed, Jacobian $(\partial E/\partial\theta_A)$ is included to obtain neutron intensity per unit energy transfer. The $S(Q, E)$ so obtained still contains the resolution broadening. Further, since the energy resolution varies across the scan, the broadening of the $S(Q, E)$ would also vary as a function of $E$. (viii) Correction due to multiple scattering in the sample has been avoided by choosing a not too thick sample (say giving about 10% single scattering). (ix) Multiphonon contribution has also to be corrected. This is estimated later in this paper.

The geometrical corrections are specific to the particular geometry used in the experiment. In our experiment, the horizontal dimension of the Cu(111) monochromator was 10 cm, the beam opening at monitor was 5 cm wide, the flat surface of the sample of 5 cm vertical × 4 cm horizontal was kept bisecting the $(180 - \theta_s)$ angle in transmission geometry and horizontal dimension of the PG(002) analyzer was 7 cm. The analyzer size of 7 cm with the fixed analyzer angle $\theta_A$ of 20·5° in the fixed $E_f$ (= 14·8 meV) case essentially restricted the useful neutron beam width intercepted by the analyzer to 2·4 cm (= 7 sin 20·5°).

Hence the correction factors associated with geometry of the experiment in fixed $E_f$ case are the following: correction factor associated with (ii) was $\cos(\theta_S/2)$, and correction factor (iii) was $[w - 0{\cdot}08(w-2)^2]$ applied only for $2 < w < 5$ cm, where $w = 10 \sin\theta_M$. The factor due to correction (iv) was $1 + 0{\cdot}88 \exp(-3E/kT)$.

$S(Q, E)$ obtained from measured intensities after applying corrections discussed above are shown in figures 4(a) and 5(a). The "neutron weighted" or the generalized density of states $g^{(n)}(E)$ is derived from $S(Q, E)$ using relation (2) given below. It differs from the true density of states $g(E)$. The partial contributions $g_k(E)$ from the different atomic species $k$ are weighted by their respective "neutron scattering weightage factors" $b_k^2/m_k$, ($b_k$ = scattering length and $m_k$ = mass of the atom $k$) to yield $g^n(E)$ (eq. 4); whereas $g(E)$ is merely a sum of the partial densities of states from each species of

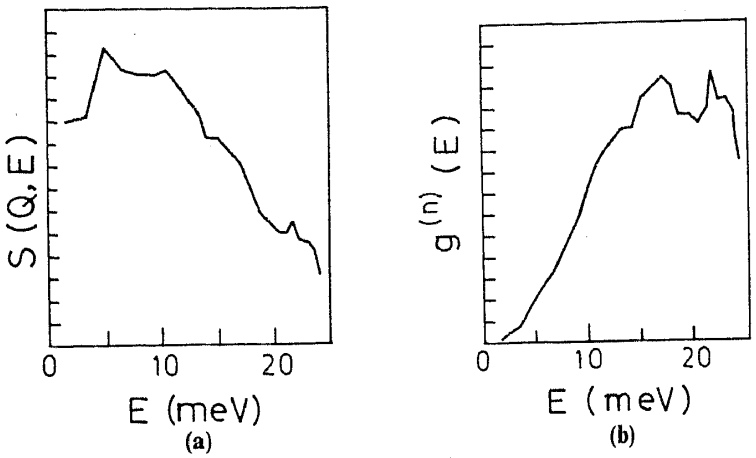


**Figure 4.** Analysis of data measured with fixed $E_i$ (shown in figure 2). The energy resolution ($\Delta E$) is about 5 meV. (**a**) $S(Q, E)$. (**b**) $g^{(n)}(E)$. $Q$ averaging has not been performed since the scattering angle was fixed; $Q$ varied between 2·9 and 3·3 $A^{-1}$.

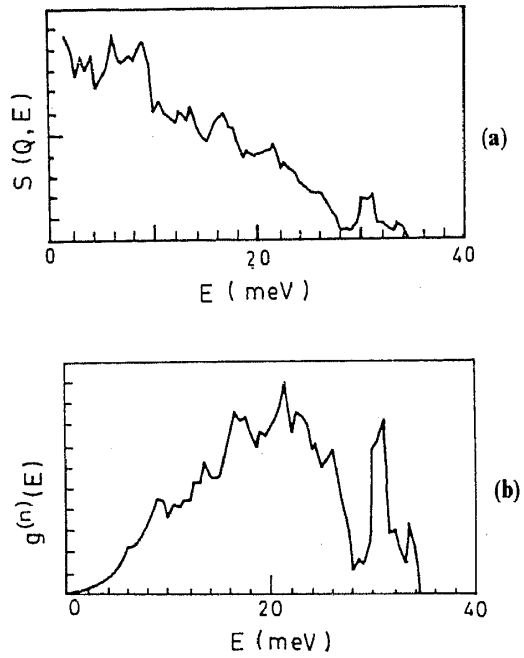


**Figure 5.** Analysis of data measured with fixed $E_f$ (shown in figure 3). The energy resolution ($\Delta E$) varied from 2 meV (at $E = 0$) to 5 meV (at $E = 35$ meV). (**a**) $S(Q, E)$. (**b**) $g^{(n)}(E)$. $Q$ averaging has not been performed. $Q$ was constant over the scan ($= 3\,A^{-1}$).

atoms (eq. 5). For the neutron energy loss experiment, we have

$$g^{(n)}(E) = S(Q, E)[E \exp(Q^2u^2)]/[Q^2\{n(E, T) + 1\}] \quad (2$$

$$n(E, T) = [\exp(E/kT) - 1]^{-1} \quad (3$$

$$g^{(n)}(E) = \sum_k g_k(E) b_k^2/m_k, \quad (4$$

$$g(E) = \sum_k g_k(E). \quad (5$$

Equation (2) is strictly true only in the "incoherent approximation", in which it i

assumed that, when summed over a large number of phonon wave vectors, the correlation between the atomic motions may be ignored. This is, however, true only for a large value of $Q$, but experiments are carried out for smaller $Q$ values for reasons of neutron intensity etc. In general, therefore, the $g^{(n)}(E)$ obtained from eq. (2) would be $Q$-dependent. In particular, the heights of the various peaks in the energy distribution would depend on $Q$ although the peak positions themselves may not change much. Data have to be obtained for a large number of $Q$ values and then a suitable averaging or extrapolation to large $Q$ can be carried out. In the present feasibility experiment we have obtained the $g^{(n)}(E)$ from two different scans, one shown in figure 4(b) from data taken with $E_i$ fixed and at constant scattering angle with $Q$ varying from 2·9 $A^{-1}$ to 3·3 $A^{-1}$, and the other shown in figure 5(b) from data taken with $E_f$ fixed and at constant $Q$ of 3 $A^{-1}$.

The $g^{(n)}(E)$ shown in figures 4(a) and 5(b) agree with each other qualitatively in the sense that the peak positions agree but the densities themselves differ from each other. We believe that these differences arise because $Q$-averaging is not performed over extensive $Q$-values. However, we note that as far as peak positions are concerned they are consistent with those in $g^{(n)}(E)$ from another data obtained by us (Chaplot *et al* 1987, 1988b) at the pulsed neutron source ISIS of the Rutherford Appleton Laboratory (UK) on a different type of instrument (TFXA) in which both $E_f$ as well as the scattering angle are kept fixed.

We have also performed a calculation of the $g^{(n)}(E)$ for comparison with the experimental data. The semi-rigid molecular model is used for the study of lattice dynamics of TCNE (Chaplot 1987 and references therein), which includes the contributions from all the intermolecular vibrations and those of the intramolecular vibrations relevant in the energy region of 0 to 40 meV. The partial phonon densities of states corresponding to each of the vibrational degrees of freedom are multiplied by the appropriate neutron scattering weightage factors and then summed over to give the total one-phonon neutron-weighted density of states $g^{(n)}(E)$. In the incoherent approximation the one-phonon part so calculated is $Q$-independent. The multiphonon contribution is separately obtained for temperature of 300 K and $Q = 3\,A^{-1}$, using Sjolander's formalism (Sjolander 1958). The calculated results are shown in figure 6 where a Gaussian broadening of FWHM of 2 meV is also included. The multiphonon contribution is seen to be quite signficant. The experimental results differ from the result of the calculation in terms of the peak heights, which may be partly due to insufficient $Q$-averaging and varying resolution broadening in the

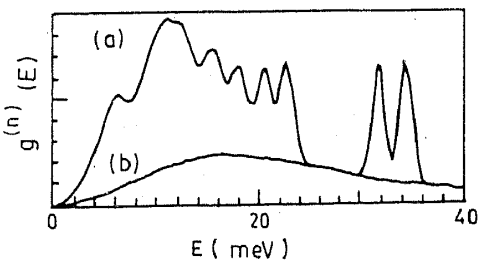


**Figure 6.** Calculation of $g^{(n)}(E)$ using a quasiharmonic semi-rigid molecular model of the intermolecular and the intramolecular vibrations up to 40 meV. For comparison with figure 5(b), we give (**a**) the total of the one phonon and the multiphonon spectrum for $Q$ of 3 $A^{-1}$ and 300 K, and (**b**) the multiphonon part of the spectrum. The one phonon calculation is in the incoherent approximation and therefore $Q$ independent.

experimental spectrum. Otherwise there is satisfactory agreement between the results of the experiment and the calculation in terms of the extent of the spectrum and the band gap near 28 meV.

## 4. Summary

In this paper we have presented the inelastic neutron scattering data from powder samples of coherently scattering tetracyanoethylene at room temperature using facilities at the Dhruva reactor. Often it is emphasized that detailed phonon dispersion relation has to be examined in the study of various phases of a solid. Such information can be obtained only from single crystal experiments. However, it is known, as also shown in a recent paper (Chaplot 1987), that the phonon density of states may also be used in the study of phase transitions via calculation of the free energy, specific heat etc. Powder samples in large quantity are easier to obtain and the phonon density of states can be rather efficiently determined as compared to the difficulty of determination of the phonon dispersion relation which requires single crystals. Such easier measurements can provide additional data in the examination of models of lattice dynamics and the interatomic potentials as shown in the present work on tetracyanoethylene. Various important corrections involved in the analysis of the measured scattering data to derive one-phonon density of states are discussed. The density of states, as derived, is found to be qualitatively in agreement with that measured experimentally at the spallation neutron source ISIS and that theoretically calculated from a lattice dynamical semi-rigid molecular model for the system.

## References

Carpenter J M and Price D L 1985 *Phys. Rev. Lett.* **54** 441

Chaplot S L 1986 *Neutron inelastic scattering, in the summer course on use of reactor neutron beams in study of materials*, course conducted under the Regional Cooperative Agreement of IAEA at Bhabha Atomic Research Centre, Bombay (unpublished)

Chaplot S L 1987 *Phys. Rev.* **B36** 8471

Chaplot S L, Chakravarthy R and Tompkinson J 1987 Annual Report of ISIS, RAL, UK page A66

Chaplot S L and Mukhopadhyay R 1986 *Phys. Rev.* **B33** 5099

Chaplot S L, Mukhopadhyay R, Vijayaraghavan P R, Deshpande A S and Rao K R 1988a *Proc. Solid State Phys. Symp.* (India) **C31** 153

Chaplot S L, Rao K R, Chakravarthy R and Tompkinson J 1988b Annual Report of ISIS, RAL, UK page A133

Dorner B 1972 *Acta Crystallogr.* **A28** 319

Maley N, Lannin J S and Price D L 1986 *Phys. Rev. Lett.* **56** 1720

Mukhopadhyay R, Chaplot S L and Rao K R 1985 *Phys. Status. Solidi.* **A92** 467

Roy A P and Brockhouse B N 1970 *Can. J. Phys.* **48** 1781

Sahu P C, Barathan R, Yousuf M, Govinda Rajan K, Mukhopadhyay R, Chaplot S L and Rao K R 1987 *Proc. Solid State Phys. Symp.* (India) **C30** 36

Sjolander A 1958 *Arkiv Fysik* **14** 315